



Scholars Research Library

Der Pharma Chemica, 2012, 4(4):1535-1543  
(<http://derpharmachemica.com/archive.html>)



ISSN 0975-413X  
CODEN (USA): PCHHAX

## A Cost Effective Approach to Prepare Pure and PEG Coated Superpara Magnetic Iron Oxide Nanoparticles by Hydrothermal Process

S. Amala Jayanthi<sup>1</sup>, A. Muthuvinayagam<sup>1</sup>, T. Manovah David<sup>2</sup> and P. Sagayaraj<sup>1\*</sup>

<sup>1</sup>Department of Physics, Loyola College, Chennai – 600 034. India.

<sup>2</sup>Department of Chemistry, Madras Christian College, Chennai – 600 059. India.

### ABSTRACT

We report a novel method to prepare monodisperse and superpara magnetic iron oxide nano particles (magnetite and maghemite) using low cost and non-toxic precursors under low temperature hydrothermal conditions. In this method,  $FeCl_3$  and  $FeCl_2 \cdot 4H_2O$  were used as iron sources and  $NH_4OH$  was added for controlling the pH value and oleic acid as dispersing agent. The synthesized particles are characterized by XRD, SEM and TEM. Their magnetic properties are studied by VSM at room temperature. The TEM results showed that the nanoparticles are monodisperse with an average size of 7-11 nm and 12-16 nm in diameter for maghemite and magnetite nanoparticles respectively. The nanoparticles are proved to be very close to super-paramagnetic with a saturation magnetization of 40.1 emu/gm and 44.75 emu/gm for magnetite and maghemite respectively. The samples exhibit very low retentivity and coercivity. The synthesized particles are coated with PEG 6000 and PEG 20,000 as a possible route to produce high magnetization polymer-coated nanoparticles for use in biomedical applications. The SEM results ascertain the surface morphology and the PEG coating. The magnetic properties of the coated nanoparticles are also studied at room temperature using VSM and they show slight increase in the saturation magnetization values. The present study demonstrates the nanoparticles formation and the controlled agglomeration by varying the polymer concentration.

**Keywords:** Nanoparticle; Iron Oxides; Super paramagnetism; PEG; Hysteresis studies.

### INTRODUCTION

Magnetic properties of fine-particle systems have assumed great importance in recent years because of their scientific and technological utility. Maghemite ( $\gamma-Fe_2O_3$ ) and magnetite ( $Fe_3O_4$ ) are commonly used in magnetic ink, as catalyst, as magnetic recording media and as ferrofluids for biomedical uses [1]. In all applications, there exists considerable incentive to decrease particle size, which generally enhances the performance. Also, these iron oxide phases behave differently in magnetic fields depending on their grain dimensions typically being ferromagnetic in the micron scale and super-paramagnetic in the nanoscale. This feature is believed to occur because of the thermal fluctuation of the direction of the magnetic moment [2].

Recent studies have demonstrated the feasibility of surface functionalized super paramagnetic iron oxide nanoparticles for use in a variety of biological applications. Magnetic nanoparticle based targeting can reduce or eliminate the side effects of conventional chemotherapy by reducing systematic distribution of drugs and lower the doses of the cytotoxic compounds [3]. The intriguing potential applications of magnetic iron oxide nanostructures have stimulated rapid development of synthetic techniques. For this reason, a variety of synthetic methods such as co-precipitation, microemulsion, sol-gel, reverse & normal micelles, ultra- sound irradiation, ball-milling, hydrothermal method, thermal decomposition of organometallic compounds, etc., have been applied to produce magnetic iron oxide nanoparticles and to realize the desired properties [4]. The major problem associated with most

of these methods is the poor control of particle size, distribution and dispersity. To address these concerns, herein we report the synthesis of monodisperse  $\gamma$  Fe<sub>2</sub>O<sub>3</sub> and Fe<sub>3</sub>O<sub>4</sub> nanoparticles using common inorganic precursors via a water-organic interface under hydrothermal conditions. We have used the hydrothermal method for the synthesis of the nanostructures because various nanostructured materials can be prepared at temperatures substantially lower than those required by conventional solid state or vapour reactions. More importantly hydrothermal processes can promote formation of crystalline products without any post treatment. The as-synthesized nanoparticles can be collected in a non-polar organic solvent from the reaction mixture simply by using a separating funnel.

Also, monodispersed particles with a high saturation magnetization values and functionalized with suitable polymers are required for targeting in hyperthermia, transfection and MRI. Several approaches have been developed to coat iron oxide nanoparticles including in-situ coatings and post-synthesis coating. For example, Josephson et al. have developed a co-precipitation process in the presence of dextran [5]. The post-synthesis coating method consists of grafting the polymer on the magnetic particles once synthesized. In the literature, the most common polymers used for coatings are dextran, polyvinyl alcohol, starch, arabinogalactan, poloxamers and polyoxamines [6]. In the present work, coating the synthesized particles with two different varieties of PEG namely PEG 6000 and PEG 20,000 for improving the suspension stability and magnetic properties is demonstrated.

## MATERIALS AND METHODS

### 2. Experimental

#### 2.1. Chemicals

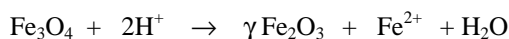
FeCl<sub>3</sub>, NH<sub>4</sub>OH, oleic acid, toluene, ethanol and chloroform were all purchased from Merck Specialties Pvt. Ltd., Mumbai. FeCl<sub>2</sub>.4H<sub>2</sub>O and PEG 6000 were purchased from LOBA CHEMIE, Pvt. Ltd., Chennai and PEG 20,000 was purchased from Spectro Chemicals Pvt. Ltd., Mumbai, and was used as received without further purification.

#### 2.2. Synthesis of $\gamma$ Fe<sub>2</sub>O<sub>3</sub> and Fe<sub>3</sub>O<sub>4</sub>

The chemical reaction of Fe<sub>3</sub>O<sub>4</sub> formation may be written as,



According to the thermodynamics of this reaction, complete precipitation of Fe<sub>3</sub>O<sub>4</sub> should be expected at a pH between 8 and 14 with a stoichiometric ratio of 2:1 (Fe<sup>3+</sup> / Fe<sup>2+</sup>) in a non-oxidizing oxygen environment [7]. However, magnetite (Fe<sub>3</sub>O<sub>4</sub>) is not very stable and is sensitive to oxidation. Magnetite is transformed into maghemite ( $\gamma$  Fe<sub>2</sub>O<sub>3</sub>) in the presence of oxygen.



Oxidation in air is not the only way to transform magnetite ( $\gamma$  Fe<sub>2</sub>O<sub>3</sub>) into maghemite, various electron or iron transfers depending upon the pH of the suspension are also involved. In the present work, FeCl<sub>3</sub> and FeCl<sub>2</sub>.4H<sub>2</sub>O were taken as the sources of Fe<sup>3+</sup> / Fe<sup>2+</sup>. The pH was adjusted to 9 by drop wise addition of ammonium hydroxide. Oleic acid dissolved in toluene was added to the above reaction mixture and the solution was then transferred to a Teflon-lined stainless steel autoclave. The temperature of the autoclave was kept at 120°C for 2 hours. The reaction mixture was then allowed to cool to room temperature naturally. A brown slurry was obtained. The product was separated by the addition of chloroform in a separating funnel. The particles were then precipitated by dissolving with ethanol and brown particles of ( $\gamma$  Fe<sub>2</sub>O<sub>3</sub>) were obtained after centrifuging and drying the precipitate at 120°C. The precipitate was thermally heated at 400°C in air atmosphere to produce black magnetite (Fe<sub>3</sub>O<sub>4</sub>) particles. Thus, the black Fe<sub>3</sub>O<sub>4</sub> and reddish brown  $\gamma$ Fe<sub>2</sub>O<sub>3</sub> nanoparticles were obtained using the same precursors.

#### 2.3. PEG Modification

The as-synthesized particles of  $\gamma$ Fe<sub>2</sub>O<sub>3</sub> and Fe<sub>3</sub>O<sub>4</sub> were surface-modified with poly ethylene glycol (PEG) which is eco-friendly, nontoxic, biocompatible and bio degradable in nature. Two different varieties of PEG namely PEG 6000 and PEG 20,000 were used for surface modification. The as prepared nanoparticles of Fe<sub>3</sub>O<sub>4</sub> and PEG 6000 were taken in 1:2 ratio and then dissolved in de-ionized water. The mixture was dispersed in an ultrasonic oscillator for 20 minutes and then the particles were separated by centrifuging and drying. The same procedure was repeated with PEG 20,000. The  $\gamma$ Fe<sub>2</sub>O<sub>3</sub> nanoparticles are also surface modified with PEG 6000 and PEG 20,000 in the same manner. These PEG modified nanostructured magnetic particles can be used as drug carriers.

## 2.4. Characterization Techniques

The powder XRD pattern for the as prepared magnetic nanoparticles was recorded by a Rich Seifert, X-ray diffractometer using monochromatic nickel filtered  $\text{CuK}\alpha$  ( $\lambda = 1.5416\text{\AA}$ ) radiation. Scanning electron microscope (SEM) was employed for morphological study using a JEOL JSM 6310 operated at 10KV with Energy Dispersive X-ray Analyzer (EDAX). TEM images were recorded on a JOEL JEM 3010 with an accelerating voltage of 200 kV. Magnetic measurements were carried out with the EG&G Princeton applied research Vibrating Sample Magnetometer (VSM) model 4500.

## RESULTS AND DISCUSSION

### 3.1. X-ray Powder Diffraction

As noted earlier, the two different phases of iron oxide  $\gamma\text{Fe}_2\text{O}_3$  and  $\text{Fe}_3\text{O}_4$  were synthesized and the crystallinity and phase purity of the samples are confirmed using X-ray diffraction. The nanosize of the synthesized particles is evident from the observed peak broadening for the spectra.

For  $\gamma\text{Fe}_2\text{O}_3$  nanoparticles peaks at  $30.1^\circ$ ,  $35.67^\circ$ ,  $43.18^\circ$ ,  $53^\circ$ ,  $57.29^\circ$  and  $62.80^\circ$  corresponding to the planes (220), (313), (400), (513) and (440) of iron oxide are identified. The crystal structure was found to be tetragonal with lattice constant  $a = 8.3879\text{\AA}$  and  $c = 23.7249\text{\AA}$  using XRDA program and these values agree well with the JCPDS (89-5894) values ( $a=8.346\text{\AA}$  and  $c = 25.034\text{\AA}$ ), thus conforming the formation of  $\gamma\text{Fe}_2\text{O}_3$ . The XRD pattern is shown in Fig. 1.

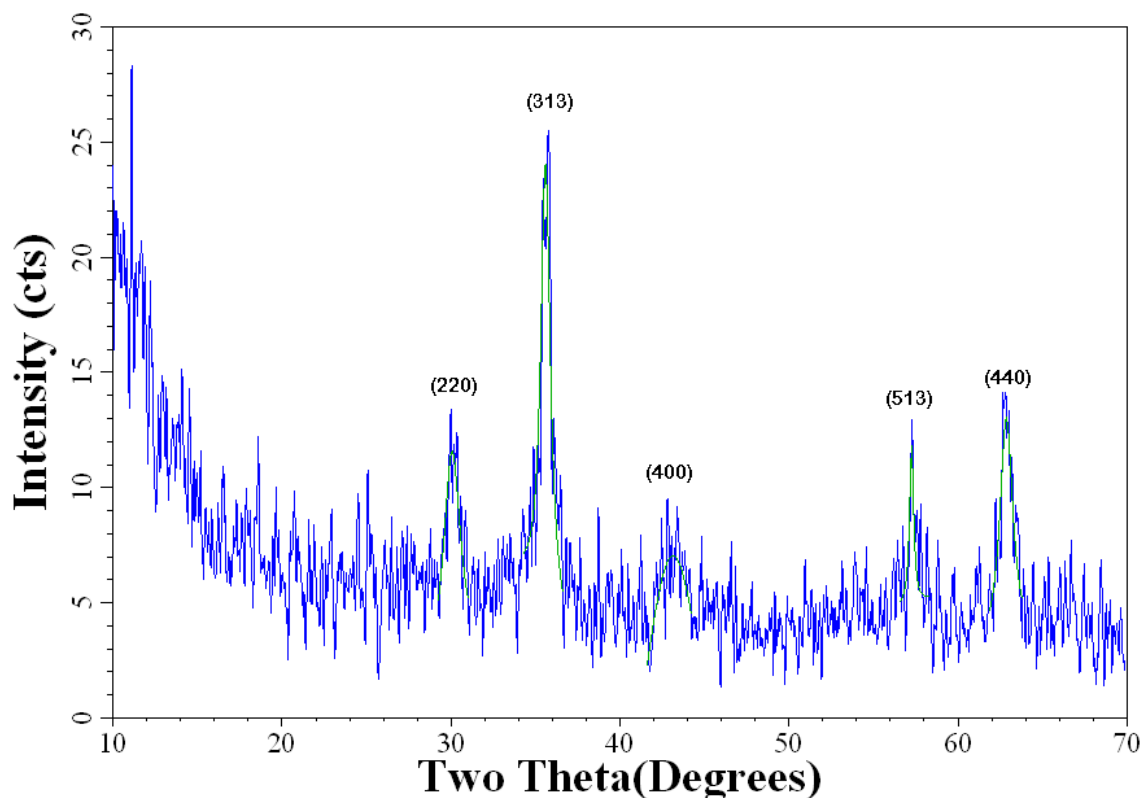


Fig. 1 XRD pattern for  $\gamma\text{Fe}_2\text{O}_3$

For  $\text{Fe}_3\text{O}_4$  particles, peaks at  $30^\circ$ ,  $35.6^\circ$ ,  $43.04^\circ$ ,  $53.1^\circ$ ,  $57.02^\circ$  and  $62.88^\circ$  corresponding to planes (220), (311), (400), (422) (511) and (440) are identified. The crystal structure was found to be cubic with lattice constant  $a = 8.4272\text{\AA}$  using XRDA program, and this matches well with JCPDS (89-3854) data ( $a=8.393\text{\AA}$ ). The pattern is shown in Fig.2.

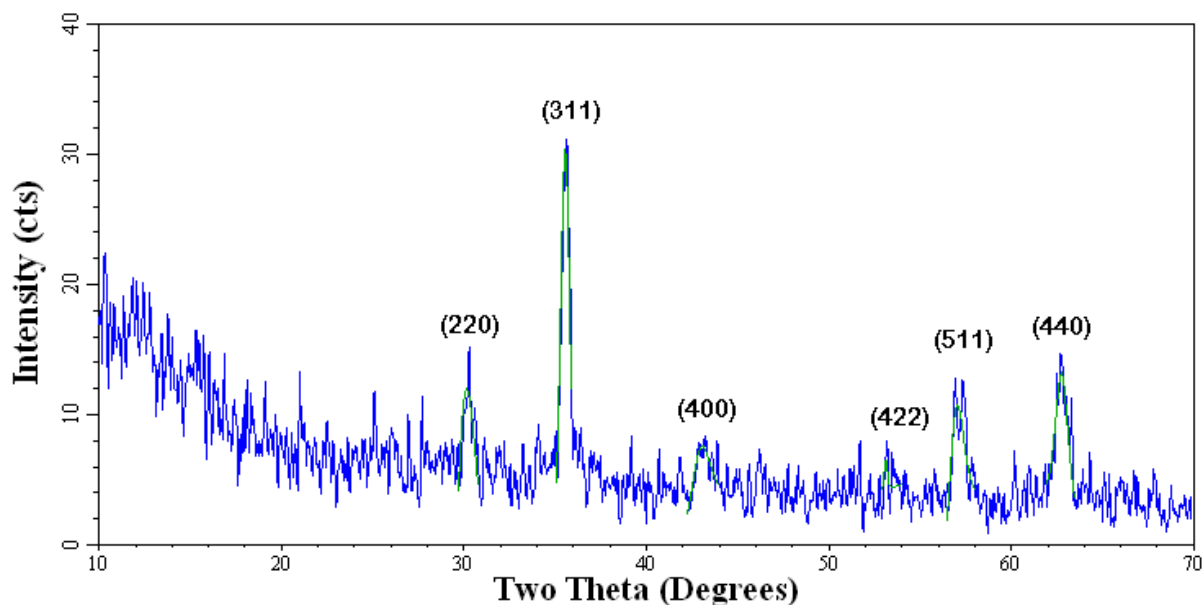


Fig. 2 XRD Pattern for  $\text{Fe}_3\text{O}_4$

The average crystallite size is calculated from the XRD line broadening using the Scherrer formula [10],

$$d = \frac{0.9\lambda}{\beta \cos \theta}$$

Where  $d$  is the diameter of the particles,  $\beta$  the half maximum line width after correcting for instrumental line broadening and  $\lambda$  is the wave length of X-rays. The average crystallite size is obtained as 13.22nm for  $\gamma\text{Fe}_2\text{O}_3$  and 14.3nm for  $\text{Fe}_3\text{O}_4$  particles using this procedure.

### 3.2. TEM analysis

Direct imaging of the individual nanocrystallites and the generation of a detailed statistical data of the size and shape of the particle in the sample was investigated using TEM. Fig. 3 and 4 show the Transmission Electron Micrograph (TEM) images of the  $\gamma\text{Fe}_2\text{O}_3$  and magnetite nanoparticles. The TEM images show that the maghemite particles are moderately monodisperse and spherical with average particle size of 11 nm. The TEM images for the magnetite particles are shown in Fig.4. It shows the spherical and monodisperse nature of the nanoparticles and the particle size is around 15 nm. This is comparable to the average crystallite size obtained from XRD analysis.

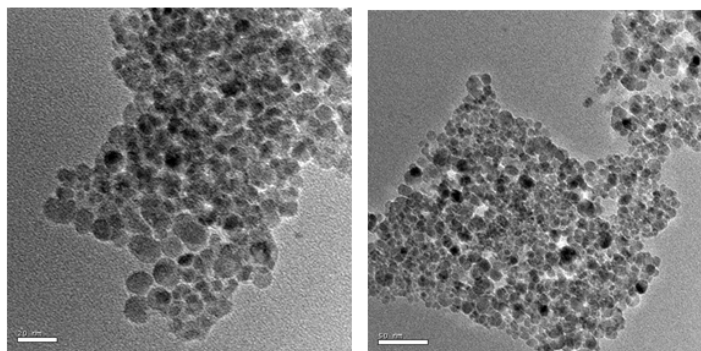


Fig. 3 TEM images of  $\gamma\text{Fe}_2\text{O}_3$

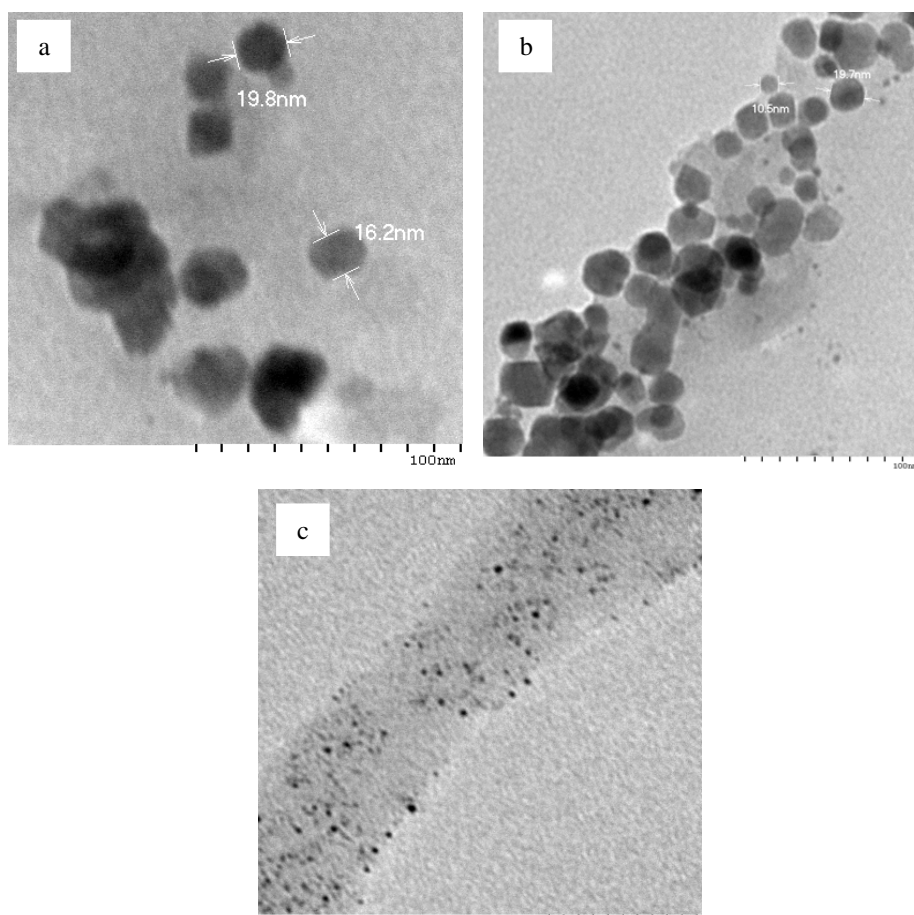
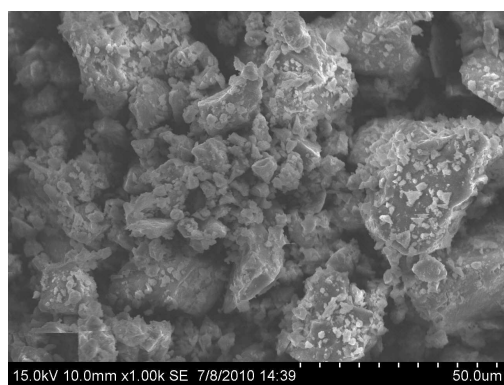


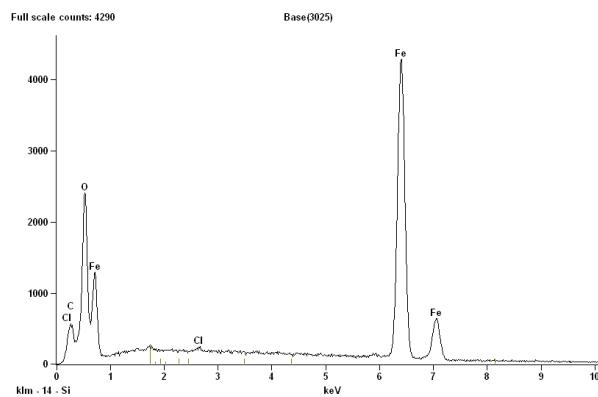
Fig. 4 TEM images of  $\text{Fe}_3\text{O}_4$

### 3.3 Scanning electron microscope (SEM) analysis:

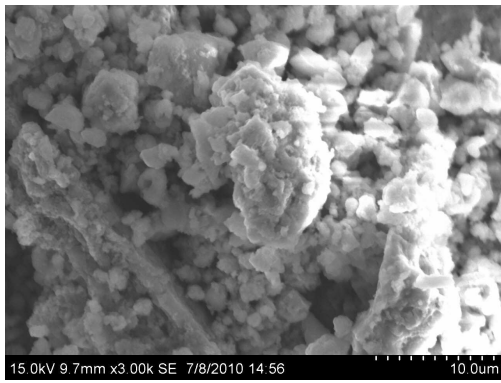
The surface morphology of the as prepared sample was examined by SEM. Fig. 4 a, b, c show the SEM images of pure  $\gamma\text{-Fe}_2\text{O}_3$  and PEG coated  $\gamma\text{-Fe}_2\text{O}_3$  particles. Fig. 5 a, b, c show the SEM images of pure  $\text{Fe}_3\text{O}_4$  and PEG coated  $\text{Fe}_3\text{O}_4$  particles. From the picture, it is clear that the uncoated particles are well monodisperse and of uniform size. EDAX spectrum for the synthesized particles indicates that iron oxide structures are composed to only Fe and O. In spite of coating with PEG, the obtained nanoparticles does not show the presence of any kind of organic impurity in it. Since the organic residuals are removed by several cycles of washing / centrifugation the EDAX spectrum shows only small quantity of Carbon in the PEG coated particles. The data confirms the high purity of the as prepared samples.



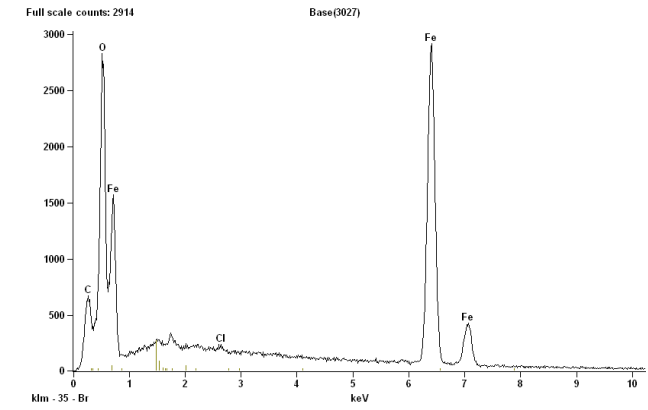
Pure Maghemite



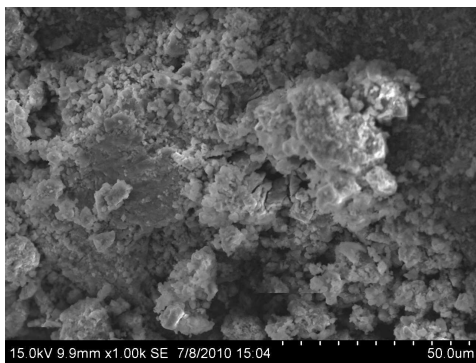
(a) EDAX Spectrum of  $\gamma\text{-Fe}_2\text{O}_3$



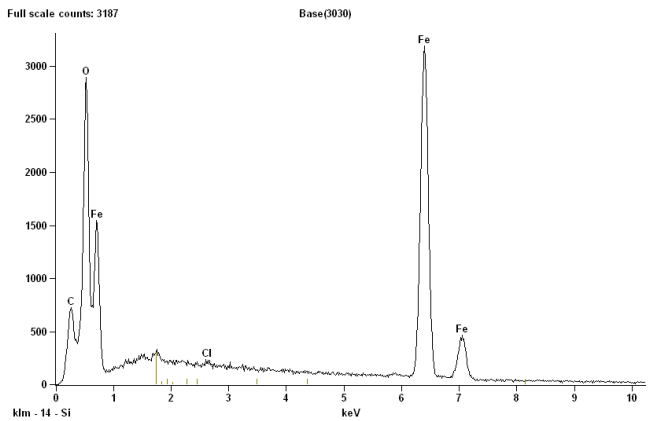
PEG 6000 coated Maghemite



(b) EDAX Spectrum of PEG 6000 coated  $\gamma$  Fe<sub>2</sub>O<sub>3</sub>

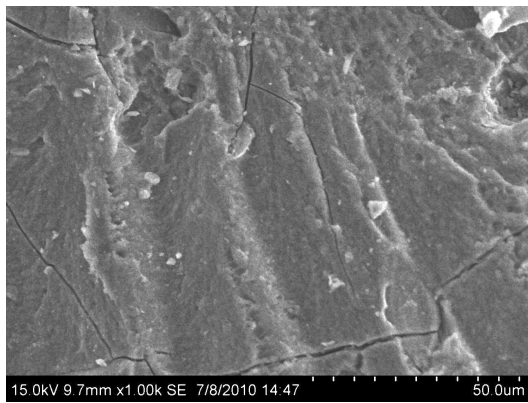


PEG 20,000 coated Maghemite

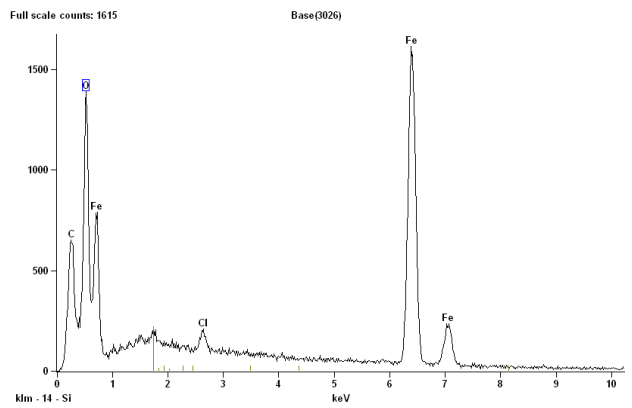


(c) EDAX Spectrum of PEG 20,000 coated  $\gamma$  Fe<sub>2</sub>O<sub>3</sub>

Fig. 4 SEM images of (a) Pure (b) PEG 6000 coated (c) PEG 20000 coated Maghemite



Pure Magnetite



(a) EDAX Spectrum of pure Fe<sub>3</sub>O<sub>4</sub>

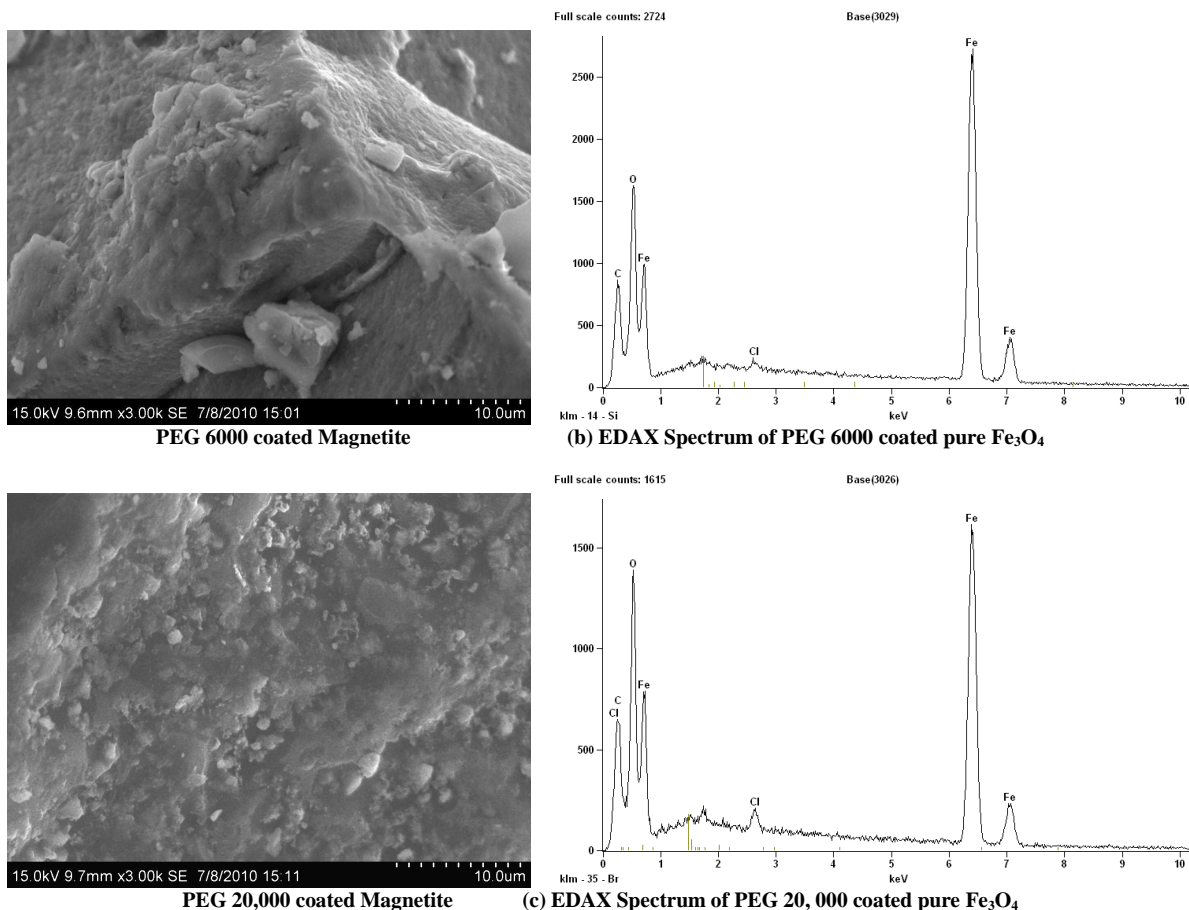
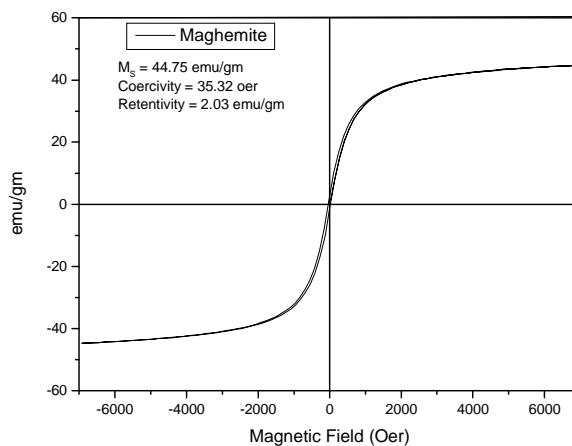


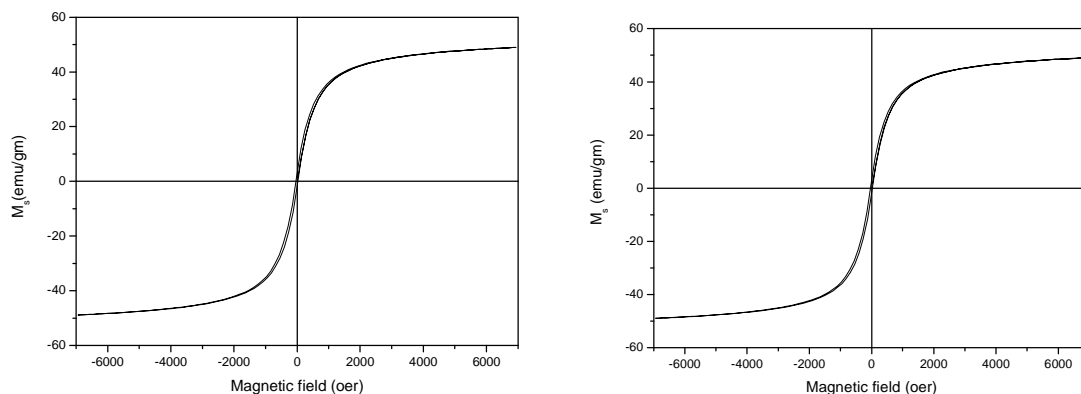
Fig. 5 SEM images of (a) Pure (b) PEG 6000 coated (c) PEG 20000 coated Magnetite

**3.4 Magnetic Properties:**

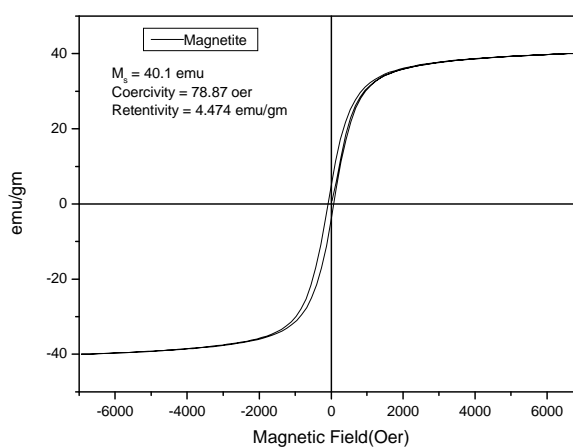
To study the magnetic properties of the synthesized magnetic nanoparticles, the room temperature magnetization hysteresis curves are measured using Vibrating Sample Magnetometer (VSM). The graphs obtained for the Pure and PEG coated magnetic nanoparticles are shown in Fig. 6 and 7.



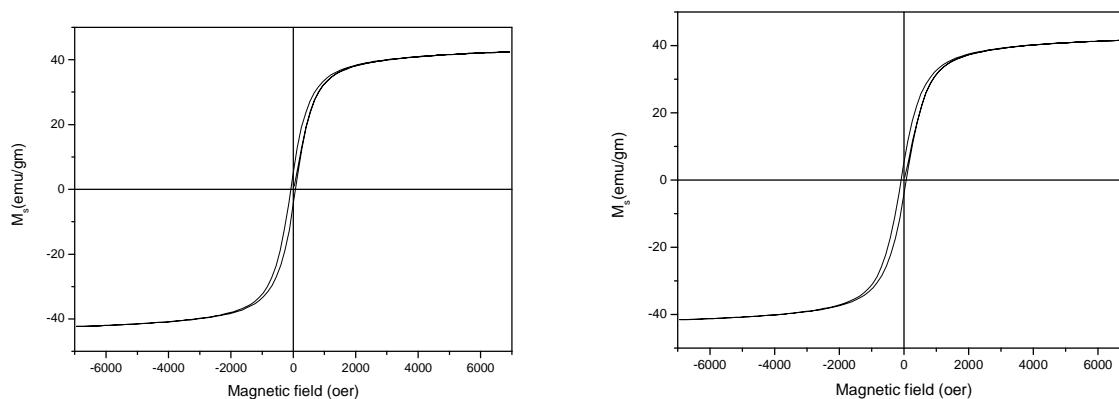
(a)



(b) (c)  
**Fig. 6 Hysteresis curves for (a) Pure (b) PEG 6000 coated (c) PEG 20000 coated Maghemite**



(a)



(b) (c)  
**Fig. 7 Hysteresis curves for (a) Pure (b) PEG 6000 coated (c) PEG 20000 coated Magnetite**

It shows that forward and backward magnetization curves of the samples are almost the same with a small hysteresis and with negligible coercivity and remanence. For  $\gamma\text{Fe}_2\text{O}_3$  (maghemite) particles, since the size is around 10nm, there is no hysteresis and the particles are superparamagnetic. For  $\text{Fe}_3\text{O}_4$  (magnetite) particles, the size calculated from TEM and XRD slightly exceeds the domain size (critical size) and they are approaching the superparamagnetic state. The saturation magnetization, coercivity and remanence values for the pure and PEG coated magnetic nanoparticles are shown in the Table 1. The  $M_s$  values for the nanoparticles are lower than the corresponding values for the bulk materials. It is suggested that as the nanoparticles possess a large surface to volume ratio, the surface disorder phase and the non-magnetic layer would reduce the magnetic behaviour of the material. Also magnetic properties of nanosized particles are largely dependent on their crystallinity.  $M_s$  decreases with decreasing crystallite size for mono-domain particles due to surface spin coating and thermal fluctuation. The detailed magnetic properties



can be elucidated only after studying the variation of susceptibility with temperature since that gives the value of Block temperature at which the transition from ferromagnetic phase to superparamagnetic state takes place.

**Table 1: Saturation magnetization, coercivity and retentivity values for the pure and PEG coated iron oxide nanoparticles**

State	Maghemite			Magnetite		
	M <sub>s</sub> emu/gm	Retentivity emu/gm	Coercivity oer	M <sub>s</sub> emu/gm	Retentivity emu/gm	Coercivity oer
Pure	44.75	2.03	35.32	40.1	4.309	78.78
PEG 6000 coated	48.96	2.316	30.65	42.42	4.995	77.32
PEG 20,000 coated	49.04	2.395	31.2	41.64	1.669	81.07

The M<sub>s</sub> values for the PEG coated  $\gamma$ -Fe<sub>2</sub>O<sub>3</sub> and Fe<sub>3</sub>O<sub>4</sub> nanoparticles increases slightly compared to their pure form. This increasing tendency of M<sub>s</sub> is consistent with the growth of the particle size and enhancement in crystallinity.

### CONCLUSION

Superparamagnetic iron oxide nanoparticles of  $\gamma$ -Fe<sub>2</sub>O<sub>3</sub> and Fe<sub>3</sub>O<sub>4</sub> were successfully synthesized by a simple, novel and cost-effective hydrothermal method. The average crystallite size calculated for  $\gamma$ -Fe<sub>2</sub>O<sub>3</sub> is 13.2nm and for Fe<sub>3</sub>O<sub>4</sub> 14.3nm from XRD peak broadening. TEM results for the  $\gamma$ -Fe<sub>2</sub>O<sub>3</sub> and magnetite nanoparticles shows that the particles are well monodisperse with a average particle size of 10 nm and 15 nm respectively. The magnetization studies at room temperature show that the  $\gamma$ -Fe<sub>2</sub>O<sub>3</sub> particles are superparamagnetic with M<sub>s</sub> value of 44.75 emu/gm. For Fe<sub>3</sub>O<sub>4</sub> nanoparticles, since the size of the particles is nearing their critical value they show slight hysteresis and are approaching superparamagnetism. The PEG coated particles show slightly improved M<sub>s</sub> values and the results are tabulated. The addition of PEG can elevate the crystallinity of the samples and changes the product morphology which causes the value of magnetic saturation increased. These PEG coated iron oxide nanoparticles synthesized in this work could be used for biomedical application as magnetic carriers or contrasting agents due to their small particle size and superparamagnetic property.

### Acknowledgement

The authors acknowledge the University Grants Commission (UGC) India for providing instrumentation facility through a Major Research Project (F.38-19/2009(SR)).

### REFERENCES

- [1] R.M. Cornell, U. Schwertmann, The Iron Oxides. Structure, Properties, Reactions and Uses, YCH : Weinheim, Germany, **2003**.
- [2] D. Vollath, D.V. Szabo, R.D. Taylor, J.O. Willis, *12* (**1997**)2175.
- [3] A.B. Matthew, L. Zhi, D.A. Paul, M. Apurva, L.G. Ronald, C.H. John, *J. Phys. Chem. C.* 112(**2008**)18399.
- [4] C.H. Gee, Y.K. Hong, D.W. Erickso, M.H. Park, *J. Appl. Phys.* 93 (**2003**)7560.
- [5] S. Palmacci, L. Josephson, E.V. Groman, U.S. Patent 6,262,176,**1995**. Chem. Abstr, 122(**1996**)309897.
- [6] Y. Zhang, N. Kohler, M. Zhang, *Biomaterials* **2002**, 231553.
- [7] D.K. Kim, Y. Zhang, J. Kehr, T. Klason, B. Bjeke, M.J. Muhammed, *Magn. Magn. Mater.* 225 (**2001**)256.
- [8] K.G. Paul, T.B. Frigo, J.Y. Groman, E.V. Groman, *Bioconjugate Chem.* 15 (**2004**), 394.
- [9] J.P. Jolivet, C. Chaneac, E. Tronc, *Chem. Commun.* 5(**2004**)481.
- [10] B.D. Cullity, S.R. Stock, Elements of X-ray Diffraction, 3<sup>rd</sup> ed., Prentice-Hall, New Jersey, (**2001**)170.